Chapter 35
Bayesian STAI Anxiety Index Predictions Based on Prefrontal Cortex NIRS Data for the Resting State

Masakaze Sato, Wakana Ishikawa, Tomohiko Suzuki, Takashi Matsumoto, Takeo Tsujii, and Kaoru Sakatani

Abstract Several distinctive activity patterns have been observed in the brain at rest. The aim of this study was to determine whether the STAI index can be predicted from changes in the oxy- and deoxy-hemoglobin (Hb) concentrations by using two-channel prefrontal cortex (PFC) NIRS data for the ***resting state***. The study population comprised 19 subjects. Each subject performed four trials, each of which consisted of resting with no task for 3 min. Data were acquired using a portable NIRS device equipped with two channels. The prediction algorithm was derived within a Bayesian machine learning framework. The prediction errors for seven subjects were not greater than 5.0. Because the STAI index varied between 20 and 80, these predictions appeared reasonable. The present method allowed prediction of mental status based on the NIRS data at resting condition obtained in the PFC.

Keywords NIRS • Prefrontal cortex • STAI anxiety index

1 Introduction

The brain in the resting state has been an active area of research in brain science [1]. In the resting state, the brain uses a significant amount of energy even when performing no task, and several distinctive activity patterns have been observed.

M. Sato (✉) • W. Ishikawa • T. Suzuki • T. Matsumoto
Department of Electrical Engineering and Bioscience, Waseda University,
3-4-1 Kasumigaoka, Lions Garden Kamifukuoka #801, Fujimono-si, Saitama 356-006, Japan
e-mail: sato09@matsumoto.eb.waseda.ac.jp

T. Tsujii • K. Sakatani
Division of Optical Brain Engineering, Department of Neurological Surgery,
Nihon University School of Medicine, Tokyo, Japan

W.J. Welch et al. (eds.), *Oxygen Transport to Tissue XXXIV*, Advances in Experimental Medicine and Biology 765, DOI 10.1007/978-1-4614-4989-8_35,

One way of classifying patterns of brain activity is to detect the network structure of the activity using the hierarchical clustering algorithm [2]. Although such studies are often conducted with fMRI data, one of the nontrivial aspects is that the dimension of the fMRI data is typically tens of thousands.

We attempted to predict the degree of anxiety of individuals from the oxy- and deoxy-hemoglobin (Hb) levels acquired from two-channel portable near infrared spectroscopy (NIRS) data for the prefrontal cortex (PFC) in the resting states. fMRI measures mainly deoxy-Hb levels while NIRS measures both deoxy- and oxy-Hb, and our algorithm incorporates both oxy- and deoxy-Hb levels. A quantification of anxiety is needed for predicting the anxiety of individuals. We considered the state-trait anxiety inventory (STAI) index. An important aspect of this research project was the prediction method. It was formulated within a Bayesian machine learning framework [3] and implemented by Markov Chain Monte Carlo (MCMC).

2 Materials and Methods

2.1 Experimental Settings

The study population comprised 19 subjects (13 women; 6 men), aged 20–24 years. All the subjects were healthy, with no past history of psychiatric or neurological disorders. The subjects gave written informed consent on forms approved by the ethical committee of the Nihon University School of Medicine.

Each subject was seated in a comfortable chair in a dimmed room, and we measured the changes in oxy- and deoxy-Hb concentration using a two-channel NIRS system (PNIRS-10, Hamamatsu Photonics K.K., Japan). The NIRS probes were set symmetrically on the forehead; the positioning is similar to the midpoint between the electrode positions Fp1/Fp3 (left) and Fp2/Fp4 (right) of the international 10–20 system.

One trial consisted of the following steps: Step 1, relaxation period 30 s; Step 2, preparation period 30 s; Step 3, analysis period 3 min. Each subject performed four trials and the STAI questionnaires were completed before the trials commenced. Figure 35.1 shows the experimental protocol.

2.2 NIRS Data

The device was capable of acquiring NIRS data through two channels; each channel consisted of oxy- and deoxy-Hb levels. The acquired data consisted of four-dimensional values collected for 4 min per task. We used the latter 3-min data for analysis. The sampling frequency was 10 Hz; thus, there were 1,800 data points for each trial. Twenty features computed from the four-dimensional data are summarized in Table 35.1.

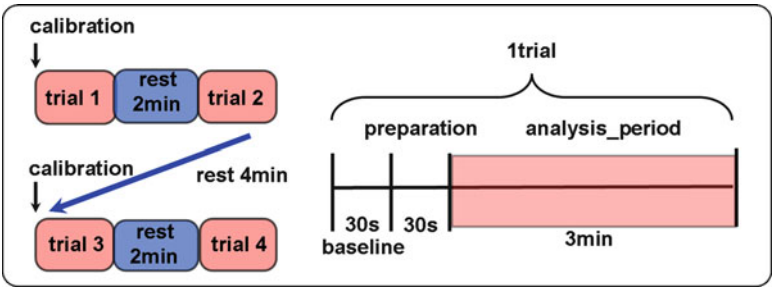

Fig. 35.1 Flow of tasks

Table 35.1 The features used in this study

No.	Mean	No.	Variance	No.	Covariance	No.	Correlation coefficient
1	Oxy(right PFC)	5	Oxy(r)	9	Oxy(r)/deoxy(r)	15	Oxy(r)/deoxy(r)
2	Deoxy(right PFC)	6	Deoxy(r)	10	Oxy(r)/oxy(l)	16	Oxy(r)/oxy(l)
3	Oxy(left PFC)	7	Oxy(l)	11	Oxy(r)/deoxy(l)	17	Oxy(r)/deoxy(l)
4	Deoxy(left PFC)	8	Deoxy(l)	12	Deoxy(r)/oxy(l)	18	Deoxy(r)/oxy(l)
–		–		13	Deoxy(r)/deoxy(l)	19	Deoxy(r)/deoxy(l)
–		–		14	Oxy(l)/deoxy(l)	20	Oxy(l)/deoxy(l)

The numbers in odd-numbered columns are feature numbers

2.3 Prediction

2.3.1 Prediction Flow

A leave-one-out prediction was conducted. Of the 76 (= 19 participants × 4 trials) data sets, one was reserved for testing, and the remaining 75 data sets and the STAI indices were used for training the machine After the parameters were learned, the reserved data were input to the machine for STAI index prediction.

2.3.2 Prediction Algorithm

Let $x_t^{(i)} := (x_{t1}^{(i)}, ..., x_{tk}^{(i)}) \in R^K$, $t = 1, ..., T$, $i = 1, ..., N$, be the NIRS feature vector for the t-th trial of the i-th individual. For raw features, $K = 20$; however, the dimension will be later reduced to three in a principled manner. Let $y^{(i)}$, $i = 1, \ldots, N$ be the STAI state index calculated from the questionnaire ($N = 19$). We attempted to fit the data with the following learning model:

$$P(y^{(i)} \mid x_t^{(i)}; \omega, \beta) = \sqrt{\frac{\beta}{2\pi}} \exp\left(-\frac{\beta}{2} (y^{(i)} - f(x_t^{(i)}; \omega)) \right)^2, \tag{35.1}$$

where f is the basis function for data fitting, and β is another unknown parameter (often called hyperparameter), which corresponds to the magnitude of uncertainty in the STAI indices. Because we expected the relationship between the NIRS data and the STAI index to contain nonlinearity, we considered the following **nonlinear** basis function:

$$f(x_t^{(i)};\omega) := \sum_{h=1}^{H}\left[\omega_{(K+1)h}\sigma\left(\sum_{k=1}^{K}[\omega_{kh}x_{tk}^{(i)}]+\omega_{0h}\right)\right]+\omega_{(K+1)0}, \tag{35.2}$$

where σ is a sigmoidal function that incorporates potential nonlinearities, and $= \{\omega_{kh}, \omega_{0h}, \omega_{(K+1)0}\}$ where $k = 1,\ldots, K+1$, $h = 1,\ldots, H$, are the unknown parameters associated with the basis function. All the unknown parameters, , needed to be learned from the available data $\{x_t^{(i)}, y^{(i)}\}$. This study formulated the prediction problem within a Bayesian framework, where a prior distribution is assumed about the unknown parameters that are incorporated into the data model given by (35.1).

The prior distribution for $_k$ was assumed to be specified by $P(\ _k|\alpha_k) = N(0,(1/\alpha_k)\boldsymbol{I})$ where $N(0,(1/\alpha_k)\boldsymbol{I})$ denotes the Gaussian distribution with a mean of 0 and a covariance matrix $(1/\alpha_k)\boldsymbol{I}$; α_k is another hyperparameter to be learned, and $\boldsymbol{I}$ denotes the H-dimensional identity matrix. This prior distribution indicates that the unknown parameters are often small in magnitude instead of large, and this fact often prevents overfitting. The prior distributions for α_k are assumed to follow the gamma distribution. In addition to the K parameter vectors $\{\ _k\}$, there were two parameters $\{\ _{0h}$, $_{(K+1)0}\}$ with which we associated another hyperparameter α_{K+1}. Let $\alpha = \{\alpha_k\}$, $x = \{x_t^{\{i\}}\}_{t,i}$, $y = \{y^{(i)}\}$. Assuming the data from each trial to be independent, the Bayes formula gives the posterior distribution:

$$P(\omega,\alpha \mid x,y,\beta) \propto \prod_{t,j} P(y^{(i)} \mid x_t^{(i)};\omega,\beta)P(\omega \mid \alpha)P(\alpha). \tag{35.3}$$

Equation (35.3) quantifies the plausibility of a particular value of the data for learning (***x; y***). Using (35.3), the prediction of the STAI index associated with the preserved data $y_{\text{preserved}}$ was performed. The calculation of (35.3) was nontrivial; therefore, we used Markov Chain Monte Carlo analysis to make approximations. This procedure was repeated 76 times while changing the data reserved for the test each time. Because the actual STAI index was available from the subject, the prediction error was computed.

We chose $H = 8$ so that the number of unknown parameters was $(K+1)H + 1 = 169$; this number was too large for the number of data sets used for training, i.e., 75. One way of automatically reducing the number of dimensions is to examine the posterior values of hyperparameter α_k in (35.3). A large α_k implies that the target quantity is concentrated around the origin; hence, this particular feature is relatively ineffective. Thus, by eliminating those features with large α_k values, one could reduce the number of features.

3 Results

The top left figure in Fig. 35.2 shows the posterior mean of the hyperparameters $\{\alpha_k\}$, $k = 1,\ldots, 20$. The top right figure in Fig. 35.2 shows the prediction errors summed over all the data sets corresponding to the full 20-dimensional feature vector, seven-dimensional feature vector consisting of 3, 15, 16, 17, 18, 19, and 20, five-dimensional feature vector consisting of 3, 15, 16, 19, and 20, three-dimensional feature vector consisting of 3, 15, and 16, and the one-dimensional feature that consists of only feature 3. The best performance appeared to be for the three-dimensional feature vector. The bottom left figure in Fig. 35.2 shows the prediction

result associated with trial 2 of all the subjects with the three-dimensional feature. The horizontal axis denotes the actual STAI index and the vertical axis denotes the predicted value.

4 Discussion

The brain under stress is an active area of research. Recently, it has been demonstrated that there is left/right asymmetry in the PFC activity during tasks involving mental stress. These activity patterns were measured using a two-channel NIRS device and correlated with the systemic stress responses of the autonomic nervous system and the HPA axis system [4]. This study went beyond investigating such asymmetry by predicting the STAI index based on the NIRS values. The 3-dimensional features extracted from the 20-dimensional features are schematically illustrated in the bottom right figure in Fig. 35.2, where, in addition to the mean oxy-Hb level in the left PFC, the correlation between the oxy-Hb levels in the left PFC and the right PFC seems to be significant. The correlation between the oxy-Hb level in the right PFC and the deoxy-Hb levels in the right PFC also appeared relevant. It is worth recalling that the STAI index varied between 20 and 80. The overall average prediction errors of the four trials for seven out of 19 subjects were no greater than 5.0. The prediction error of subject 17 was 1.09. For one subject, larger prediction errors were observed with the proposed algorithm. This subject had the highest STAI index of 60 in the questionnaire session. Because this is the only subject with such a high STAI index, more data are needed for elucidation. The errors associated with the remaining subjects were between 5.0 and 10.0.

If considerably more data were available, and if the proposed prediction was functional, one possible application of this study could be to help a clinician or a researcher assess the degree of anxiety of an individual, even if the target individual did not respond truthfully to the STAI questionnaire.

Acknowledgments This research was partly supported by the Japan Science and Technology Agency, under the Strategic Promotion of Innovative Research and Development Program, and a Grant-in-Aid from the Ministry of Education, Culture, Sports, Science and Technology of Japan (B23300247).

References

1. Gusnard D, Akbudak E, Shulman G, Raichle M (2001) PNAS 98:4259–4264
2. Salvador R, Suckling J, Coleman MR, Pickard JD, Menon D, Bullmore E (2005) Cereb Cortex 15:1332–1342
3. Bishop C (2006) Pattern recognition and machine learning. Springer, Berlin
4. Tanida M, Katsuyama M, Sakatani K (2007) Brain Res 1184:210–216